Effects of Torrefaction on Hemicellulose Chemical Structure in Cell Walls of Japanese Cedar

Yoshikazu Mori,[a,*] Mifu Fujiswa,[a] Takahiro Yoshida,[b] and Makoto Kiguchi [a]

*Corresponding author: mori.yoshikazu@nihon-u.ac.jp

DOI: 10.15376/biores.21.1.1548-1563

GRAPHICAL ABSTRACT

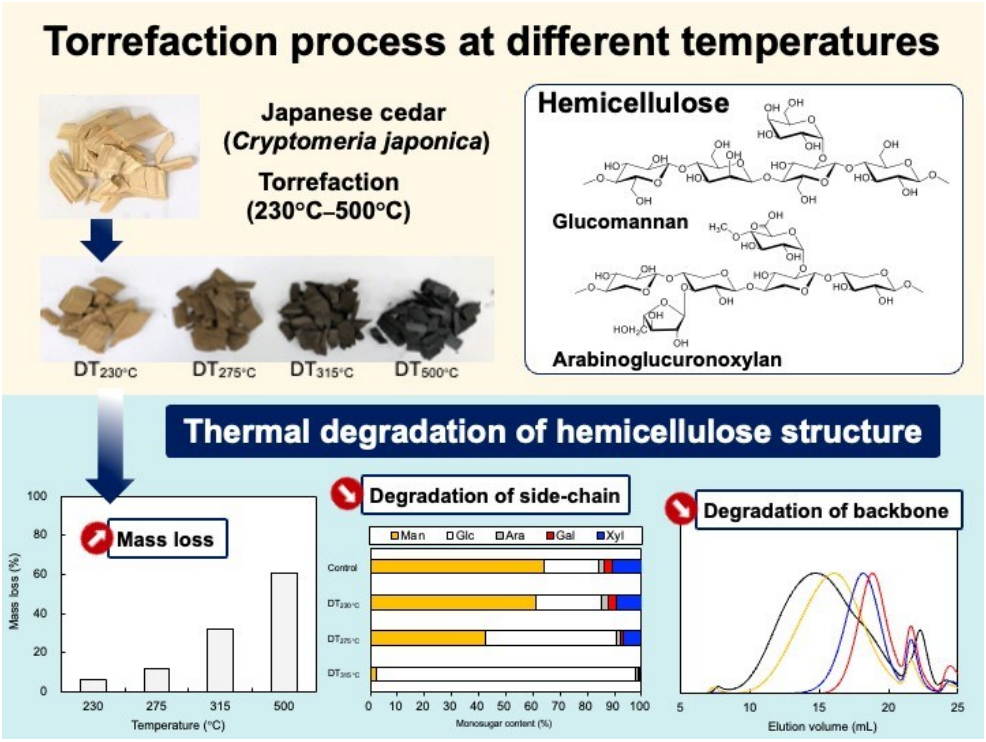

Effects of Torrefaction on Hemicellulose Chemical Structure in Cell Walls of Japanese Cedar

Yoshikazu Mori,[a,*] Mifu Fujiswa,[a] Takahiro Yoshida,[b] and Makoto Kiguchi [a]

Torrefaction is a promising technique for improving the thermochemical characteristics, including calorific value and hydrophobicity, of wood pellets. These properties of torrefied pellets are attributed to the degradation of the cell wall polymers, such as the hemicellulose structure, during the torrefaction process. This study investigated the effects of torrefaction on the chemical components of the cell wall polymers and hemicellulose structure in Japanese cedar. Wood chips were subjected to torrefaction at different temperatures (230 to 500 ºC) and characterized using various techniques, such as thermogravimetric analysis, Fourier transform infrared spectroscopy, and liquid chromatography. The torrefied samples exhibited lower hemicellulose content (glucomannan/galacto-glucomannan (GM/GGM) and arabinoglucuronoxylan (AGX)) than the control sample. In addition, the hemicellulose content of the cell wall decreased with increasing torrefaction temperature. The GM/GGM-to-AGX ratio remarkably changed after torrefaction. As the torrefaction temperature increased, high-molecular-weight assemblies of GM/GGM and AGX shifted toward low-molecular-weight assemblies. Furthermore, the side-chain structure and molecular-weight distribution of AGX decomposed at a lower torrefaction temperature (230 °C), indicating that the AGX polymeric structure had lower thermal stability than GM/GGM. These results provide information concerning the thermal degradation of the behavior of each hemicellulose polymeric structure during the torrefaction.

DOI: 10.15376/biores.21.1.1548-1563

Keywords: Japanese cedar; Torrefaction; Wood cell wall; Hemicellulose; Glucomannan; Arabinoglucuronoxylan; Thermal stability

*Contact information: a: College of Bioresource Sciences, Nihon University, 1866 Kameino, Fujisawa, Kanagawa 252-0880, Japan; b: Forestry and Forest Products Research Institute, 1 Matsunosato, Tsukuba, Ibaraki 305-8687, Japan; *Corresponding author: mori.yoshikazu@nihon-u.ac.jp*

INTRODUCTION

Woody biomass is a widely available renewable energy feedstock that provides approximately 10% of the global primary energy demand. Japanese cedar (*Cryptomeria japonica* D.Don) is one of the most important softwood species in Japan, and its large-dimension lumber has recently been used for both residential and non-residential buildings (Annual Report on Forest and Forestry in Japan, 2023). In addition to the traditional use of raw timbers for building materials, there is an increasing demand for wood pellets for biomass energy production (Pradhan *et al.* 2018; Zaini *et al.* 2021). Wood pellets exhibit higher energy densities and lower moisture content than ordinary wood chips and are easier to handle (Yoshida *et al.* 2013). However, they have disadvantages, such as lower energy density than fossil fuels, weak hydrophobic properties, and the tendency to swell and lose

their shape when saturated with water (Larsson *et al.* 2013; Yoshida *et al*. 2013; Tumuluru 2018).

In biomass conversion, torrefaction has attracted attention as a promising pretreatment technique for improving conventional wood pellets (Eseltine *et al*. 2013; Cahyanti *et al.* 2020; Kota *et al*. 2022). The torrefaction process involves a milder heat treatment than conventional carbonization, and the general target temperature range before the occurrence of severe thermal degradation is 200 to 300 °C (Prins *et al*. 2006; Eseltine *et al*. 2013; Shoulaifar *et al*. 2014; Stirling *et al*. 2018; Cahyanti *et al*. 2020; Kota *et al*. 2022). Torrefaction can improve the thermochemical characteristics such as calorific value and hydrophobic properties of wood pellets compared with the conventional process (Yoshida *et al*. 2013). The thermochemical properties of the torrefied pellets are attributed to the thermal degradation of the cell wall chemical components, such as cellulose, hemicellulose, and lignin, during torrefaction. Among the cell wall polymers, hemicellulose is more susceptible to torrefaction because of its amorphous and hydrophilic properties compared with those of the other main cell wall components (Werner *et al*. 2014; Li *et al*. 2016; Wang *et al.* 2016). During the torrefaction at about 200 °C, the polymer structure of the hemicellulose starts to decompose, and such changes increase significantly at about 250 °C, corresponding to the generation of oligomeric fragments (Shoulaifar *et al.* 2014). Then, the degradation of lignin and cellulose structures become significant at higher torrefaction temperatures and treatment duration, resulting in the more difficult formability and brittleness of torrefied pellets (Saleh *et al.* 2013; Wang *et al.* 2020). Moreover, some studies indicated that the decomposition of cell wall polymers during torrefaction leads to a reduction in their binding properties (*e.g*. hydrogen bonding ability) to the wood cell wall matrix, suggesting an impact on the formability of pellets (Prins *et al.* 2006; Larsson *et al.* 2013; Pelaez-Samaniego *et al.* 2014).

Hemicellulose in Japanese cedar is composed of heteropolysaccharides, including glucomannan/galactoglucomannan (GM/GGM) and arabinoglucuronoxylan (AGX). In particular, GM/GGM comprises approximately 70% of hemicellulose and plays an essential role as a binding agent between cellulose microfibril molecules and lignin during wood cell wall formation (Terashima *et al.* 2009). The cited authors reported that hemicellulose plays a key role in cell wall formation, including the aggregation of cellulose microfibrils *via* weak bonds (*e.g.*, hydrogen bonds and electrostatic interactions) between cellulose and hemicellulose molecules. The effects of torrefaction on the hemicellulose chemical structure have been studied through thermogravimetric analysis (TGA) and differential thermal analysis (Wang *et al.* 2016; Wang *et al.* 2020; Wang *et al*. 2021). In addition, oligomers and monosaccharides derived from hemicellulose in wood cell walls have been determined under different torrefaction conditions based on quantification and composition analysis (Garrote *et al*. 1999; Wang *et al*. 2019). Studies on hemicellulose after wood torrefaction have focused only on the quantification and elemental composition analysis of oligomers or monosaccharides (Lin *et al*. 2022). Previous studies have examined the effects of torrefaction on Japanese cedar in detail, including TGA, moisture content adjustment, and the formability of torrefied biomass (Yoshida *et al.* 2013; Yoshida *et al.* 2017). However, the changes in the hemicellulose polymeric structure of Japanese cedar after torrefaction have not been studied.

The goal of this study was to investigate the effects of torrefaction on the cell wall chemical components of Japanese cedar, particularly the chemical structure of the hemicellulose, such as GM/GGM and AGX. First, the thermochemical characteristics of the torrefied wood samples was analyzed by TGA. Fourier transform infrared (FT-IR)

spectroscopy was then employed to characterize the samples that were torrefied at different temperatures (230 to 315 °C) and carbonized at 500 °C. Then, the cell wall chemical components (lignin and holocellulose) and neutral sugar composition of the wood samples were determined. In addition, the polymeric structures of the GM/GGM and AGX (*e.g.*, sugar composition and molecular weight distribution) from the torrefied samples were evaluated. This study provides valuable insights into the hemicellulose structure in the cell wall of Japanese cedar after torrefaction.

EXPERIMENTAL

Wood Material and Reagents

Japanese cedar softwood (*Cryptomeria japonica* D. Don) was used in the form of cut chips. Monosaccharides, including glucose (Glc, 98%), mannose (Man, 98%), galactose (Gal, 99%), xylose (Xyl, 98%), and arabinose (Ara, 98%), were purchased from Wako Pure Chemical Industry Co. (Osaka, Japan). Sodium chlorite (99%) and ethanolamine monohydrate (99%) were purchased from Sigma-Aldrich Chemical Co. (St. Louis, USA). All reagents and solvents were used as received.

Methods

Torrefaction process

Air-dried wood chips of Japanese cedar (approximately 400 g) were torrefied in an inert-gas oven (Advantech Toyo Corp., Tokyo, Japan) or carbonized in a muffle furnace (Advantech Toyo Corp., Tokyo, Japan) under nitrogen flow. The torrefaction temperature was varied within the range 230 to 315 °C. The test samples included the air-dried sample (control), samples subjected to dry torrefaction (DT) at 230 to 315 °C (denoted as $DT_{230\,°C}$, $DT_{275\,°C}$, and $DT_{315\,°C}$), and a sample carbonized at 500 °C (denoted $DT_{500\,°C}$). After maintaining the torrefaction temperature for approximately 5 min, the oven was slowly cooled to room temperature (25 °C) (Yoshida *et al*. 2013, 2017).

Color measurement

Color changes in the samples were measured using an NF555 spectrophotometer (Nippon Denshoku Corp., Tokyo, Japan; D65 standard illuminant). The CIELab parameters of lightness (L^*) and color parameters (a^* and b^*) on the surface of each sample were measured. The average color parameters were obtained from three specimens of each treatment sample. The total color change (ΔE), L^*, a^*, and b^* were collected and processed using ColorMate software (Yang *et al.* 2022).

Thermal properties of the torrefied wood samples

The thermal property of the wood samples was measured by thermogravimetry (TG, Type 8122, Rigaku, Tokyo, Japan). For each experiment, 7 to 10 mg of wood powder ground to <150 μm was heated from room temperature to 800 °C at a rate of 10 °C/min under nitrogen flow. The sample mass was recorded as a function of temperature and was reported on a dry basis.

FT-IR analysis

The FT-IR spectra of the torrefied samples were obtained using an FT/IR6600 instrument (JASCO, Tokyo, Japan) equipped with an attenuated total reflectance (ATR;

ATR PRO ONE VIEW, JASCO, Tokyo, Japan) sampling tool attached to a diamond crystal. The FT-IR spectra of each wood powder were measured after the removal of the extractives using a mixture of ethanol and toluene (ethanol:toluene = 1:2, (v/v)). Each spectrum was obtained by accumulating 64 scans in an absorbance range of 4,000 to 500 cm^{-1}. Each sample was measured three times, and the average values were recorded. The band at 1,424 cm^{-1}, which corresponds to the cellulose (–C–H) stretching vibration, was used for calibration. The presence of extractives in the cell walls is indicated by changes in the IR absorption spectra of the aromatic skeleton and lignin (Mori *et al.* 2023).

Determination of chemical components

The lignin contents of the wood samples were determined using the Klason method (Yeh *et al*. 2004). The holocellulose contents of the control and DT samples were measured using the Wise method (Japan Wood Research Society 1985). High-performance liquid chromatography (HPLC) was performed using a Shimadzu LC-20AT instrument (Shimadzu, Kyoto, Japan) with a TSK-gel Sugar AX1 column (Tosoh, Tokyo, Japan) and a Shimadzu SPD-20A UV detector (310 nm, Shimadzu, Kyoto, Japan) to determine the relative sugar composition in the Klason lignin hydrolysate (Nakamura *et al*. 1999). The mobile phase, 50 mM boric acid buffer (pH 7.8) containing 0.5% ethanolamine hydrochloric acid, was eluted at a flow rate of 0.35 mL/min. The relative percentages were calculated electronically in duplicate experiments. The cellulose and hemicellulose contents were calculated as follows: cellulose (%) = Glc − (1/3 × Man) (Jones *et al*. 2006). The hemicellulose content (%) was calculated as the sum of the Ara, Gal, Glc, Man, and Xyl cellulose. The GM/GGM and AGX contents of the wood samples were calculated by assuming a fixed ratio of the relevant sugar units in each type of polysaccharide (Kibblewhite *et al*. 2010). All measurements were performed twice, and the average values were recorded.

Preparation of AGX and GM/GGM from holocellulose

Holocellulose was prepared from the control and DT samples using the Wise method. The degreased wood sample (10 g) was mixed with 280 mL deionized water and treated with sodium chlorite (4 g) and acetic acid (0.8 mL) at 80 °C for 1 h. After four successive treatments, the solid residue was recovered by filtration, washed with deionized water and acetone, and dried in a vacuum oven at 40 °C. The holocellulose thus obtained was successively extracted with hot water (65 °C) to remove GGM (Hashi *et al.* 1970). The AGX was isolated from the holocellulose after GGM extraction using a 10% potassium hydroxide aqueous solution in the presence of barium hydroxide (Kurata *et al.* 2018). The alkaline soluble fraction obtained by filtration was adjusted to pH 6 by adding glacial acetic acid, dialyzed against ion-exchanged water, concentrated, and then freeze-dried. The residue was stirred in 10% acetic acid for 2 h to neutralize the pH. During the AGX preparation, the precipitate resulting from the addition of 10% aqueous potassium hydroxide was collected *via* centrifugation. The sugar compositions of AGX and GM/GGM were determined by HPLC using a TSK-gel Sugar AX1 column after hydrolysis in 2 M trifluoroacetic acid at 120 °C for 2 h (Nakamura *et al*. 1999).

Analysis of molecular weight distribution

The molecular weights of the alkaline extractives were analyzed by size exclusion chromatography using a Shimadzu LC-10AD instrument (Shimadzu, Kyoto, Japan) and an ERC RefractoMax 520 refractive index detector (IDEX Health and Science, Tokyo, Japan)

equipped with a Superose 6 10/300 column (GE Healthcare, USA). The mobile phase of 50 mM sodium acetate buffer (pH 5.8) was eluted at a rate of 0.5 mL/min. The molecular weight distribution (M_w), degree of polymerization, and polydispersity index (PDI) were determined from a calibration curve obtained using dextran standards (M_w = 410,000, 50,000, and 12,000; Sigma-Aldrich) (Brown *et al.* 2009; Mori *et al.* 2023).

RESULTS AND DISCUSSION

Effect of Torrefaction Conditions

To investigate the changes in the chemical structure of hemicellulose and cell wall structure of woody biomass induced by torrefaction, several wood samples from Japanese cedar were torrefied at different temperatures (230 to 500 °C). Figure 1 shows the mass losses of the samples torrefied at different temperatures. The samples subjected to torrefaction at 230 and 275 °C showed a low mass loss (6.5% to 11.9%) compared with the mass of the raw biomass (dry basis). In contrast, the sample torrefied at 315 °C exhibited a high mass loss of 32.2%, indicating that the cell wall chemical components degraded to an increasing extent as the torrefaction temperature was increased.

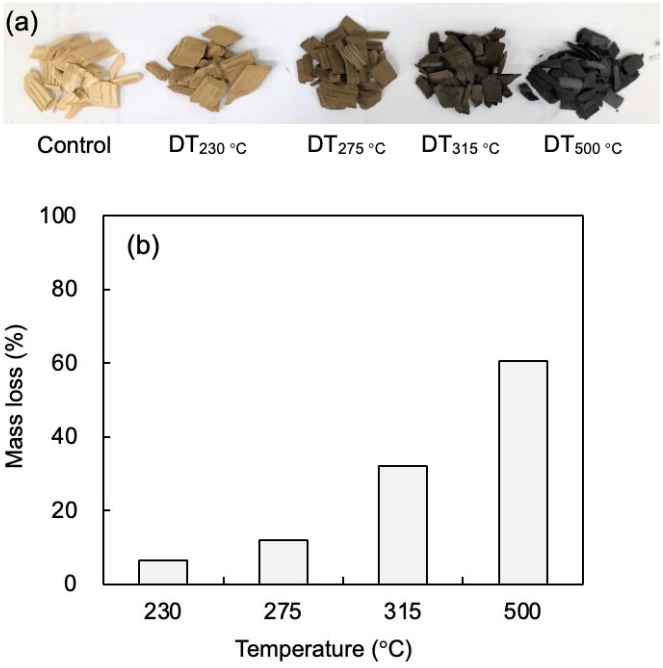

Fig. 1. (a) Torrefied Japanese cedar samples and (b) their mass loss (%) after torrefaction

During torrefaction, the mass loss and color differences of the woody biomass are related to the change in its energy density (Yoshida *et al.* 2013). The color parameters of the torrefied samples (L^*, a^*, b^*, and ΔE) were determined based on the CIELab color parameters. As listed in Table 1, the L^* value of the samples decreased, and they became darker as the torrefaction temperature increased. The distinct darkening of the wood materials with increasing torrefaction temperature can be attributed to changes in the component of the cell walls. The changes attributed to the thermal treatment of the wood materials are consistent with the results of a previous study (Kubojima *et al*. 2017). These

changes indicate the degradation of polysaccharides, including cellulose and hemicellulose, and an increase in the acid-insoluble residue content following torrefaction.

Table 1. Changes in the Color Parameters of the Torrefied Samples

Samples	Color Parameters			
	*L**	*a**	*b**	Δ*E*
Control	70.9 (0.4)	5.0 (0.1)	23.4 (0.1)	-
$DT_{230\ °C}$	53.6 (1.0)	9.6 (0.4)	24.7 (0.2)	23.8 (0.7)
$DT_{275\ °C}$	36.0 (0.1)	10.4 (0.4)	18.4 (0.6)	36.0 (0.2)
$DT_{315\ °C}$	26.3 (1.2)	5.5 (0.2)	10.1 (0.3)	46.9 (1.3)
$DT_{500\ °C}$	16.0 (2.2)	−2.7 (2.2)	−2.0 (3.9)	63.9 (3.9)

The data include the average and standard deviation (in parenthesis) of the values from three independent experiments.

Thermal Property of the Torrefied Samples

The thermal property of the wood samples after torrefaction at 230 to 500 °C was determined. Figure 2 shows the TG curves of the torrefied samples and the thermal decomposition temperature ($T_{d5\%}$) value at which the initial mass decreased by 5%. The mass loss in the control, $DT_{230\ °C}$, and $DT_{275\ °C}$ samples began at approximately 250 °C. However, the $T_{d5\%}$ value of $DT_{315\ °C}$ was higher than that of the other samples. The thermal degradation of cell wall carbohydrates involves various reactions, such as dehydration, depolymerization, and condensation (Tumuluru 2018). The TG profile of $DT_{500\ °C}$ remained largely stable up to 800 °C, indicating that the thermal decomposition of cell wall constituents—such as cellulose, hemicellulose, and lignin—had already resulted in char formation. These results indicate that the thermal stability of the torrefied samples was enhanced by the degradation of the cell wall polysaccharides, such as cellulose and hemicellulose, during torrefaction because hemicellulose is the most susceptible to thermal reactivity among the cell wall chemical components (Wang *et al.* 2016; Kudo *et al*. 2019; Wang *et al*. 2020; Wang *et al*. 2021; Sajid *et al*. 2022).

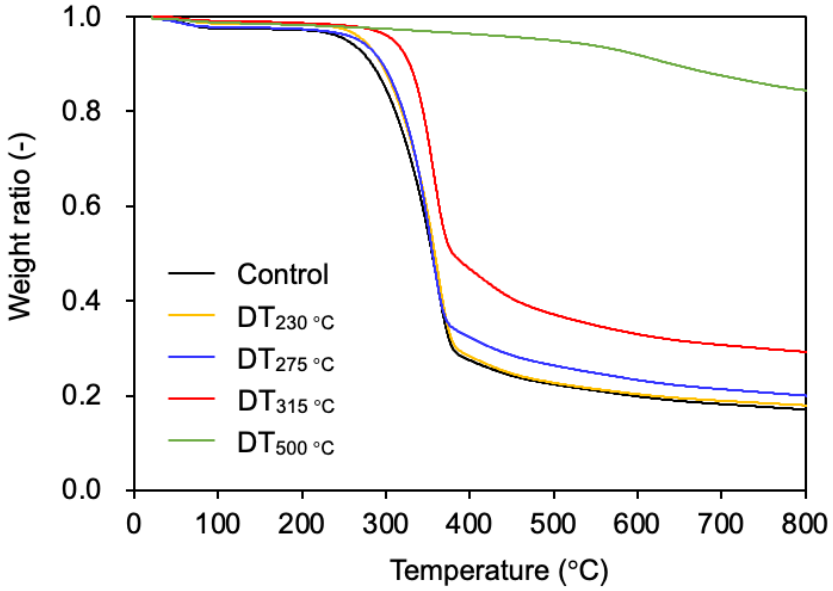

Fig. 2. Thermogravimetric curves of the torrefied samples

FT-IR Spectra of the Torrefied Samples

To investigate the chemical changes in the components of the cell walls of the samples after torrefaction, the ATR FT-IR spectra of the control and DT samples were measured. As shown in Fig. 3, both the control and DT samples showed a broad absorption band near 3300 cm^{-1}, which is attributed to the stretching vibration of the hydrogen bonds, indicating the presence of the hydroxy group in the cell wall. However, for $DT_{275\,°C}$ and $DT_{315\,°C}$, the intensity of the peak at approximately 3000 to 3600 cm^{-1} slightly decreased, indicating that the hydrophobicity was influenced by the torrefaction temperature and the carbonization of low-molecular-weight compounds (Ibrahim *et al.* 2013; Granados *et al*. 2017).

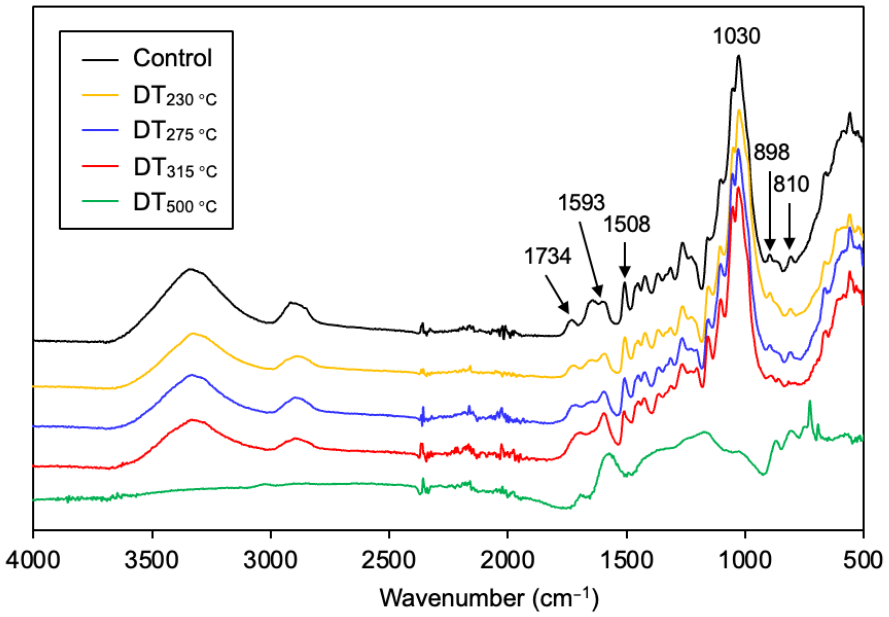

Fig. 3. Attenuated total reflectance Fourier transform infrared spectra of the torrefied samples

Considering the hemicellulose structure, the absorbance peak in the FT-IR spectra at 1734 cm^{-1}, which is attributed to the C=O stretching of unconjugated groups, was examined because it reflects changes in the carbonyl and ester groups derived from the acetyl group and glucuronic acid of hemicellulose, respectively. For $DT_{235\,°C}$ and $DT_{275\,°C}$, the relative intensity of the 1734 cm^{-1} band was only slightly changed. However, for the $DT_{315\,°C}$ sample, the absorbance peak shifted toward lower wavenumbers because of the significant degradation of AGX. This was attributed to the presence of ester or deacetylation of the C=O structure. The intensity of the GM/GGM-derived absorption band at 810 cm^{-1}, which corresponds to the ring stretching of the Man residues, decreased significantly with increasing torrefaction temperature. The decrease in the absorption of Man, which constitutes the main chain of GM/GGM, demonstrated that GM/GGM in the cell wall degraded at high torrefaction temperatures. Therefore, torrefaction strongly affected the chemical properties of hemicellulose. Furthermore, the intensities of the bands at 898 and 1030 cm^{-1}, which correspond to cell wall polysaccharides, decreased with increasing torrefaction temperature. For the cellulose structure in the cell wall framework, all samples showed similar bands at 1424 and 1368 cm^{-1}, which were ascribed to $-CH_2$ wagging vibrations and $-CH_2$ scissor motion in cellulose, respectively. However, the

intensity of the 1368 cm^{-1}, which corresponds to the C–H bending vibrations of cellulose, slightly changed at 275 °C, indicating partial decomposition of the cellulose structure.

The intensities of the lignin-derived bands at 1508 and 1596 cm^{-1} only changed slightly as the torrefaction temperature increased from 230 to 275 °C. The intensity of the 1508 cm^{-1} band, which corresponds to the vibration of the aromatic skeleton, slightly changed, whereas that of the 1596 cm^{-1} band, which is assigned to the C=O stretching vibration, remarkably increased, indicating the partial degradation of the lignin structure with increasing torrefaction temperature. These changes indicate that torrefaction at temperatures up to 275 °C promotes the degradation of cellulose and hemicellulose rather than lignin. In contrast, at 315 °C, further thermal degradation of polysaccharides and the skeletal structure of lignin was observed (Granados *et al*. 2017).

Klason Lignin Content of the Torrefied Samples

When the Klason method is used to determine the lignin content of torrefied samples, the lignin content is overestimated because of the increased insoluble content from sulfuric acid hydrolysis. The Klason lignin content is highly related to the degradation of chemical components during torrefaction. To accurately determine the lignin content in the torrefied samples, the intensity ratio of the IR absorbance (1508/1030 cm^{-1}) corresponding to the aromatic skeleton vibration from lignin in the wood cell walls was used in this study. As shown in Fig. 4, the Klason lignin contents of $DT_{230\ °C}$ and $DT_{275\ °C}$ were 30.0% and 35.2%, respectively.

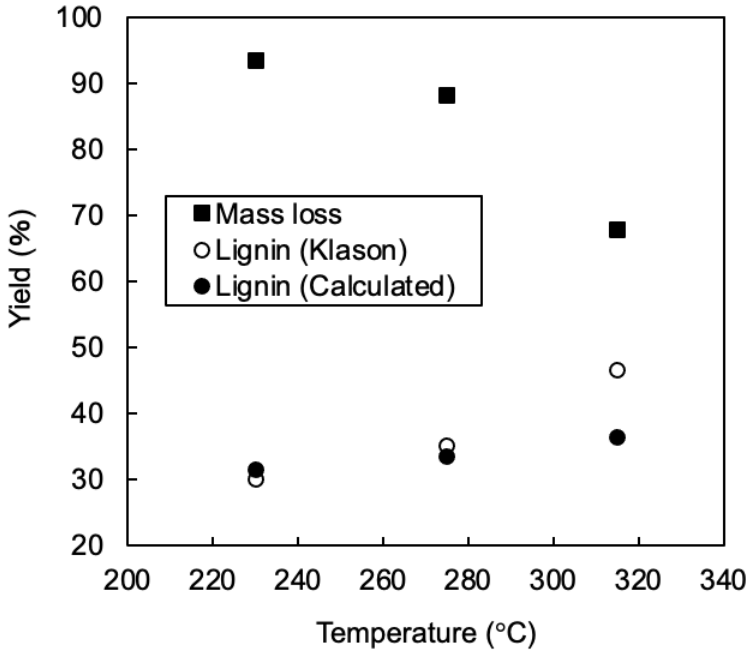

Fig. 4. Difference between the lignin contents calculated using the Klason method and the IR absorbance ratio. Results represent the average of the values from two independent experiments.

As the torrefaction temperature was increased to 315 °C, the Klason lignin content increased by 15.5% compared with that of the control sample. Compared with that of the control sample, the lignin content of $DT_{275\ °C}$ calculated using the ratio of FT-IR absorbance increased by 1.74%, whereas that of $DT_{315\ °C}$ increased by approximately 10%. These

results demonstrate that the difference in the Klason lignin content between the torrefied samples above 280 °C can be attributed to the degradation of the lignin backbone structure observed in the FT-IR spectra. Furthermore, torrefaction at temperatures above 315 °C degraded the cell wall polysaccharides (*e.g.*, cellulose and hemicellulose) and produced large amounts of acid-insoluble condensation products derived from lignin and polysaccharide condensates, indicating that the Klason lignin content calculated using the Klason lignin method had been overestimated. The extent of hemicellulose degradation increased remarkably at a torrefaction temperature of approximately 250 °C, whereas lignin degradation was minimal at this temperature.

Changes in Holocellulose Content and Neutral Sugar Composition

To examine the changes in the cell wall polysaccharides in the samples after torrefaction, the holocellulose content of the control and DT samples torrefied at 230 to 315 °C were determined using the Wise method (Table 2).

Table 2. Changes in the Chemical Components of the Cell Walls of the Samples

Samples	Polymers in the Cell Wall (%)				
	Holocellulose	Cellulose[a]	Hemicellulose[a]	GM/GGM[b]	AGX[b]
Control	72.6	49.8	22.8	62.9	37.1
$DT_{230\ °C}$	66.9	46.3	20.6	63.4	36.6
$DT_{275\ °C}$	54.5	39.8	14.7	63.8	36.2
$DT_{315\ °C}$	47.4	36.7	10.7	62.1	37.9
$DT_{500\ °C}$	N. D.	N. D.	N. D.	N. D.	N. D.

Results represent the average of the values from two independent experiments. [a] Percentage in holocellulose. [b] Percentage in hemicellulose; N.D.: not detected.

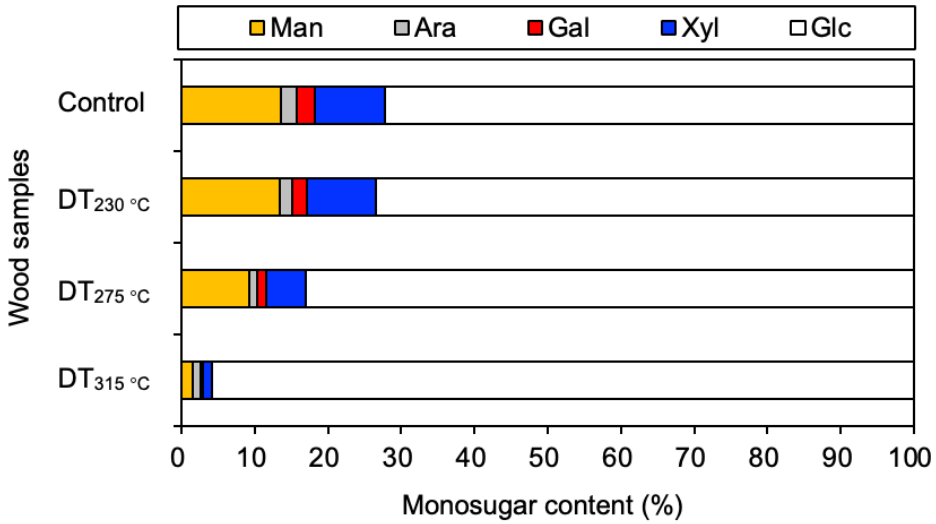

Fig. 5. Relative neutral sugar composition in the control and DT samples. The results represent the averages of values from two independent experiments.

The holocellulose content of $DT_{230\ °C}$ was slightly lower than that of the control sample. The holocellulose content decreased markedly as the torrefaction temperature increased. The proportion of hemicellulose in the holocellulose fraction was 14.7% and

10.7% for $DT_{275\ °C}$ and $DT_{315\ °C}$, respectively, indicating increased hemicellulose degradation with increasing torrefaction temperatures. In contrast, the proportions of GM/GGM and AGX in the holocellulose only changed slightly with increasing torrefaction temperature. As shown in Fig. 5, there were no Man and Xyl sugar moieties in the $DT_{315\ °C}$ sample, and the residue was mainly composed of Glc. These results indicate that hemicellulose thermally decomposed at approximately 280 °C. In addition, the amount of holocellulose in the cell walls and the hemicellulose content of wood can be expected to play a key role in the formability of torrefaction pellets.

Changes in the GM/GGM Chemical Structure

The isolated GM/GGM from the holocellulose in the control and torrefied samples were analyzed for the neutral sugar composition (Fig. 6). In general, GM consists of approximately three Man residues per Glc residue, and a Gal residue is sometimes linked to the GM/GGM backbone (Kim *et al*. 2010). The mean ratio of Man, Glc, and Gal (Man:Glc:Gal) in the GM polymer was 3:1:0.1 for the control and $DT_{230\ °C}$ samples, 2.6:1:0.2 for $DT_{275\ °C}$, and 1:1:0 for $DT_{315\ °C}$, indicating that the ratios in the GM/GGM backbone were significantly affected by torrefaction at higher temperatures.

Figure 7 shows the molecular chain-length composition, degree of polymerization, and PDI of GM/GGM in the control and DT samples. In the control sample, GM/GGM exhibited a unimodal molecular weight distribution (M_w = about 120,000) with a PDI of 3.37. The molecular weight distribution of GM/GGM in $DT_{230\ °C}$ was similar to that of the control sample. However, the degree of polymerization and PDI in $DT_{275\ °C}$ and $DT_{315\ °C}$ samples remarkably decreased, indicating the cleavage of Man and Glc linked by β-(1→4) glycosidic bonds in the GM backbone. In addition, the decomposition of the GM/GGM polymeric structure, which could not be observed in the quantitative changes in the major chemical components, had already occurred during torrefaction at 235 °C.

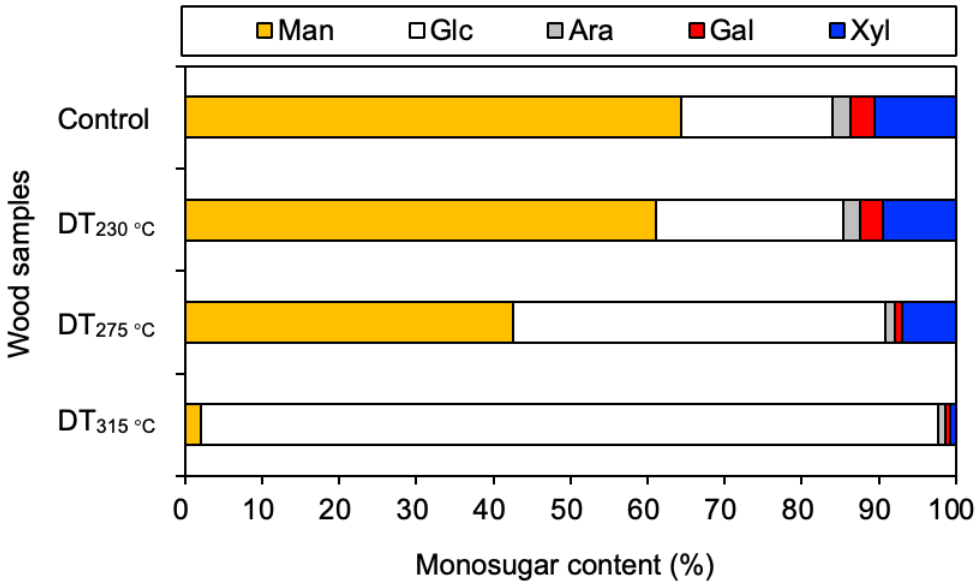

Fig. 6. Neutral sugar composition of GM/GGM in each sample. The data represent the average of the values obtained from two independent experiments. The sugar composition of the GM/GGM fraction was described as the alkaline-soluble fraction determined by HPLC analysis.

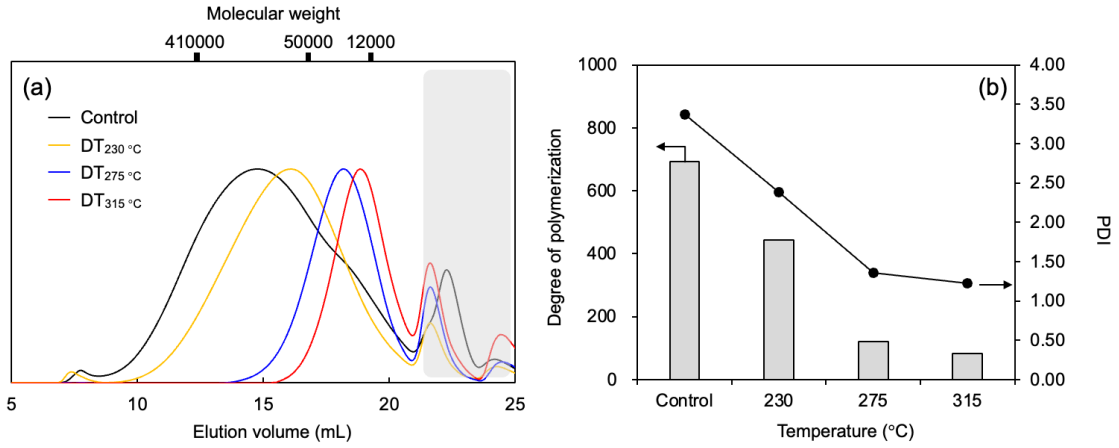

Fig. 7. (a) Molecular weight distribution and (b) degree of polymerization and PDI of GM/GGM. The gray zone represents salts in the exclusion volume.

Changes in the Chemical Structure of GM/GGM

To examine the effect of the torrefaction temperature on the AGX chemical structure, the next step was to isolate AGX from the control and DT samples and to determine the mean rate of Ara side-chain substitution in AGX (Fig. 8). The mean rate of Ara side-chain substitution in the control sample, as determined through neutral sugar analysis, was 8.5 units per 100 Xyl units. The ratios of Ara side-chain substitution in AGX for $DT_{275\,°C}$ and $DT_{315\,°C}$ were 10.2 and 20.8 units per 100 Xyl backbone units, respectively. Interestingly, the AGX fraction extracted from $DT_{275\,°C}$ contained high amounts of Glc and Man residues, in addition to the monosaccharides that comprise AGX. The Glc content derived from GM/GGM or cellulose from $DT_{275\,°C}$ may have been extracted using an aqueous alkaline solution. A previous study reported noncellulosic saccharides after the thermal treatment of wood materials (Sikora *et al.* 2018). The present results indicate that high-temperature torrefaction generates GM/GGM in the wood cell walls, which can be easily extracted using an alkaline aqueous solution.

Figure 9 shows the AGX accumulated in the control sample, comprising long-chain molecular assemblies (M_w = about 120,000) and short-chain molecules (M_w = about 12,000). Unlike the molecular weight distribution of GM/GGM, the long-chain-length assemblies of AGX decreased and shifted to a low-molecular-weight fraction of approximately 50,000 as the torrefaction temperature was increased from 230 to 235 °C. These results indicate the cleavage of the xylan backbone linked by β-(1→4) glycosidic bonds and Ara side chains in AGX under thermal degradation. At a torrefaction temperature of 235 °C, AGX began to decompose into its corresponding oligomeric fragments, after which its side chains were hydrolyzed. Considering the neutral sugar content of AGX, the chain-length composition of AGX in the DT samples may contain GM/GGM produced during the thermal degradation of the samples. Several studies have reported that the thermal stability of xylan is lower than that of GM/GGM (Shafizadeh *et al*. 1972; Werner *et al*. 2014). The present results demonstrate that the depolymerization of the AGX backbone caused by thermal degradation was greater than that of the GM/GGM backbone, which is consistent with previous reports. Due to the decomposition of the macromolecular structure in hemicellulose, the torrefaction process at higher temperatures may dramatically alter the interactions between cell wall polymers in cell walls *via* weak

bonds, such as hydrogen bonds and electrostatic interactions. This indicates a decrease in the formability of the pellet during pelletization.

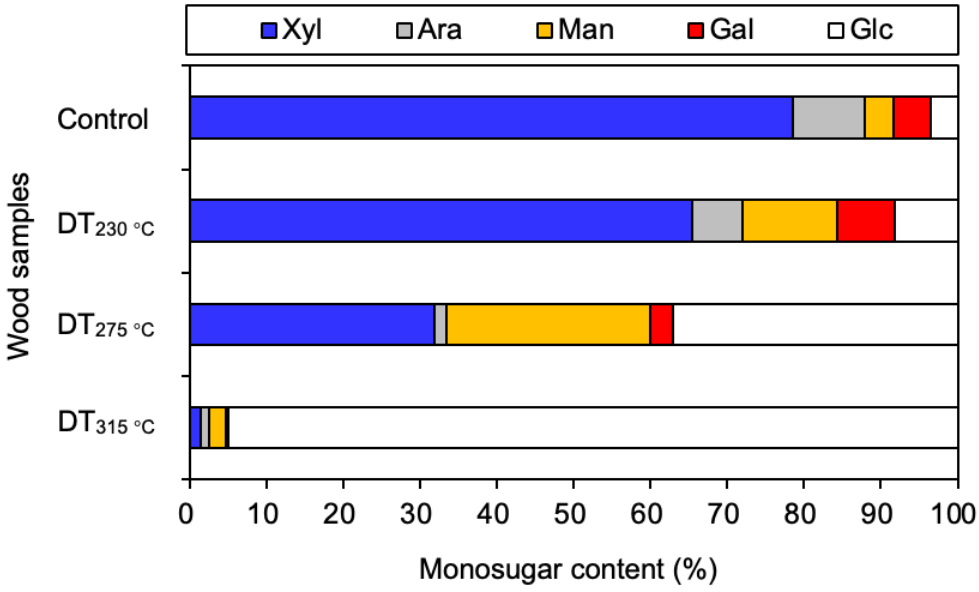

Fig. 8. (a) Neutral sugar composition of arabinoglucuronoxylan in the samples. The data represent the average values of two values obtained from independent experiments. The sugar composition in the AGX fraction was described as the alkaline-soluble fraction determined *via* HPLC analysis.

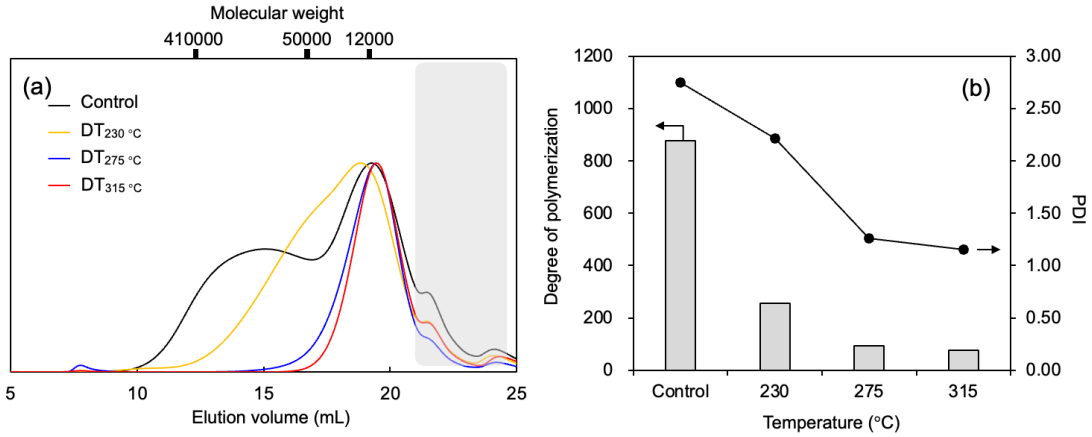

Fig. 9. (a) Molecular weight distribution and (b) degree of polymerization and PDI of AGX. The gray zone indicates salts in the exclusion volume.

CONCLUSIONS

In this study, the effects of torrefaction on the cell wall chemical components (lignin, cellulose, and hemicellulose) and thermal properties of Japanese cedar were examined. In addition, the polymeric structure and properties of hemicellulose (GM/GGM and AGX) in the cell wall were also assessed. The results are summarized as follows:

1. The thermogravimetry (TG) revealed that the thermal decomposition of hemicellulose contributed to the high thermal stability of the torrefied samples.
2. As the torrefaction temperature increased, the amount of holocellulose decreased remarkably, and the GM/GGM-to-AGX ratio in the hemicellulose fraction changed.

Furthermore, an increase in the torrefaction temperature accelerated the degradation of the chemical structure of hemicellulose.

3. At a low torrefaction temperature (230 °C), dehydration of the hydroxy group and partial decomposition of the backbone and side-chain structures in GM/GGM and AGX were mainly observed. In contrast, at higher temperatures, further depolymerization of the GM/GGM and AGX backbones and fragmentation of the sugar residues occurred.
4. These results suggest that the torrefaction of Japanese cedar accelerates the degradation of hemicellulose in its cell wall, and the polymeric structures of GM/GGM and AGX are remarkably altered in the temperature range of 230 °C to 315 °C. Therefore, the change in the macromolecular structure of hemicellulose during torrefaction might affect the brittleness and hardness in pelletizing of torrefied pellets.

ACKNOWLEDGMENTS

The authors are grateful to Kohta Miyamoto and Yasushi Hiramatsu from the Forestry and Forest Products Research Institute for providing wood samples.

Declarations of conflict of interests

The authors declare that they have no conflicts of interest.

REFERENCES CITED

Brown, D. M., Zhang, Z., Stephens, E., Dupree, P., and Turner, S. R. (2009). "Characterization of IRX10 and IRX10-like reveals an essential role in glucuronoxylan biosynthesis in *Arabidopsis*," *Plant Journal* 57(4), 732-746. https://doi.org/10.1111/j.1365-313X.2008.03729.x

Cahyanti, M. N., Doddapaneni, T. R. K. C., and Kikas, T. (2020). "Biomass torrefaction: An overview on process parameters, economic and environmental aspects and recent advancements," *Bioresource Technology* 301, article 122737. https://doi.org/10.1016/j.biortech.2020.122737

Eseltine, D., Thanapal, S. S., Annamalai, K., and Ranjan, D. (2013). "Torrefaction of woody biomass (Juniper and Mesquite) using inert and non-inert gases," *Fuel* 113, 379-388. https://doi.org/10.1016/j.fuel.2013.04.085

Garrote, G., Domínguez, H., and Parajó, J. C. (1999). "Mild autohydrolysis: An environmentally friendly technology for xylooligosaccharide production from wood," *Journal of Chemical Technology and Biotechnology* 74(11), 1101-1109. https://doi.org/10.1002/(SICI)1097-4660(199911)74

Granados, D. A., Ruiz, R. A., Vega, L. Y., and Chejne, F. (2017). "Study of reactivity reduction in sugarcane bagasse as consequence of a torrefaction process," *Energy* 139, 818-827. https://doi.org/10.1016/j.energy.2017.08.013

Hashi, M., Teratani, F., and Miyazaki, K. (1970). "Studies on hemicellulose. 2. Purification of galactoglucomannan of Japanese larch (*Larix leptolepis* Gord)," *Mokuzai Gakkaishi* 16(1), 37-41.

Ibrahim, R. H. H., Darvell, L. I., Jones, J. M., and Williams, A. (2013). "Physicochemical characterization of torrefied biomass," *Journal of Analytical and Applied Pyrolysis* 103, 21-30. https://doi.org/10.1016/j.jaap.2012.10.004

Japan Wood Research Society. (1985). "Experimental note of wood science II. Chemistry version (in Japanese)," *Japan Wood Research Society*, Tokyo.

Japan Forest Agency. (2023). "Annual Report on Forest and Forestry in Japan," *Japan Forest Agency*, Tokyo.

Jones, P. D., Schimleck, L. R., Peter, G. F., Daniels, R. F., and Clark, A. (2006). "Nondestructive estimation of wood chemical composition of sections of radial wood strips by diffuse reflectance near infrared spectroscopy," *Wood Science and Technology* 40, 709-720. https://doi.org/10.1007/s00226-006-0085-6

Kota, K. B., Shenbagaraj, S., Sharma, P. K., Sharma, A. K., Ghodke, P. K., and Chen, W. H. (2022). "Biomass torrefaction: An overview of process and technology assessment based on global readiness level," *Fuel* 324, article 124663. https://doi.org/10.1016/j.fuel.2022.124663

Kibblewhite, R. P., Suckling, I. D., Evans, R., Grace, J. C., and Riddell, M. J. C. (2010). "Lignin and carbohydrate variation with earlywood, latewood, and compression wood content of bent and straight ramets of a radiata pine clone," *Holzforschung* 64(1), 101-109. https://doi.org/10.1515/hf.2010.016

Kim, J. S., Awano, T., Yoshinaga, A., and Takabe, K. (2010). "Immunolocalization and structural variations of xylan in differentiating earlywood tracheid cell walls of *Cryptomeria japonica*," *Planta* 232, 817-824. https://doi.org/10.1007/s00425-010-1225-7

Larsson, S. H., Rudolfsson, M., Nordwaeger, M., Olofsson, I., and Samuelsson, R. (2013). "Effects of moisture content, torrefaction temperature, and die temperature in pilot scale pelletizing of torrefied Norway spruce," *Applied Energy* 102, 827-832. https://doi.org/10.1016/j.apenergy.2012.08.046

Kubojima, Y., Yanagida, T., Yoshida, T., and Kiguchi, M. (2017). "Simple estimation method for determining weight reduction in torrefied wood chips by color data," *Mokuzai Gakkaishi* 63(4), 176-182. https://doi.org/10.2488/jwrs.63.176

Kudo, S., Okada, J., Ikeda, S., Yoshida, T., Asano, S., and Hayashi, J. (2019). "Improvement of pelletability of woody biomass by torrefaction under pressurized steam," *Energy Fuels* 33(11), 11253-11262. https://doi.org/10.1021/acs.energyfuels.9b02939

Kurata, Y., Mori, Y., Ishida, A., Nakajima, M., Ito, N., Hamada, M., Yamashita, K., Fujiwara, T., Tonosaki, M., and Katayama, Y. (2018). "Variation in hemicellulose structure and assembly in the cell wall associated with the transition from earlywood to latewood in *Cryptomeria japonica*," *Journal of Wood Chemistry and Technology* 38, 254-263. https://doi.org/10.1080/02773813.2018.1434206

Li, L., Wang, X., and Wu, F. (2016). "Chemical analysis of densification, drying, and heat treatment of Scots pine (*Pinus sylvestris* L.) through a hot-pressing process," *BioResources* 11(2), 3856-3874. https://doi.org/10.15376/biores.11.2.3856-3874

Lin, Y., Chen, W., Colin, B., P´etrissans, A., Quirino, R. L., P´etrissans, M., Garrote, G., Domínguez, H., and Parajó, J. C. (2022). "Thermodegradation characterization of hardwoods and softwoods in torrefaction and transition zone between torrefaction and pyrolysis," *Fuel* 310, article 122281. https://doi.org/10.1016/j.fuel.2021.122281

Mori, Y., Suzuki, R., Yamashita, K., Katayama, Y., and Kiguchi M. (2023). "Influence of hydrothermal treatment on hemicellulose structure in *Cryptomeria japonica*," *BioResources* 18(2), 3254-3266. https://doi.org/10.15376/biores.18.2.3254-3266

Nakamura, A., Hatanaka, C., and Nagamatsu, Y. (1999). "Ultraviolet spectrometric determination of neutral monosaccharides by HPLC with ethanolamine," *Bioscience, Biotechnology, and Biochemistry* 63(7), 178-180. https://doi.org/10.1271/bbb.64.178

Pradhan, P., Mahajani, S. M., and Arora, A. (2018). "Production and utilization of fuel pellets from biomass. A review," *Fuel Processing Technology* 181, 215-232. https://doi.org/10.1016/j.fuproc.2018.09.021

Pelaez-Samaniego, M. R., Yadama, V., Garcia-Pereza, M., Lowelle, E., and McDonald, A. G. (2014). "Effect of temperature during wood torrefaction on the formation of lignin liquid intermediates," *Journal of Analytical and Applied Pyrolysis* 109, 222-233. https://doi.org/10.1016/j.jaap.2014.07.009

Prins, M. J., Ptasinski, K. J., and Janssen, F. J. J. G. (2006). "Torrefaction of wood: Part 2. Analysis of products," *Journal of Analytical and Applied Pyrolysis* 77, 35-40. https://doi.org/10.1016/j.jaap.2006.01.001

Sajid, R., Al-Abdeli, Y. M., Oluwoye, I., and Mohammednoor, A. (2022). "Torrefaction of densified woody biomass: The effect of pellet size on thermochemical and thermophysical characteristics," *BioEnergy Research* 15, 544-558. https://doi.org/10.1007/s12155-021-10319-8

Saleh, S. B., Hansen, B. B., Jensen, P. A., and Dam-Johansen, K. (2013). "Influence of biomass chemical properties on torrefaction characteristics," *Energy & Fuels* 27, 7541-7548. DOI: 10.1021/ef401569a

Shafizadeh, F., McGinnis, G. D., and Philpot, C. W. (1972). "Thermal degradation of xylan and related model compounds," *Carbohydrate Research* 25(1), 23-33. https://doi.org/10.1016/S0008-6215(00)82742-1

Shoulaifar, T. K., DeMartini, N., Willför, S., Pranovich, A., Smeds, A. I., Virtanen, T. A. P., Maunu, S., Verhoeff, F., Kiel, J. H. A., and Hupa, M. (2014). "Impact of torrefaction on the chemical structure of birch wood," *Energy and Fuels* 28, 3863-3872. https://doi.org/10.1021/ef5004683

Sikora, A., Kačík, F., Gaff, M., Vondrová, V., Bubeníková, T., and Kubovský, I. (2018). "Impact of thermal modification on color and chemical changes of spruce and oak wood," *Journal of Wood Science* 64, 406-416. https://doi.org/10.1007/s10086-018-1721-0

Stirling, R. J., Snape, C. E., and Meredith, W. (2018). "The impact of hydrothermal carbonisation on the char reactivity of biomass," *Fuel Processing Technology* 177, 152-158. https://doi.org/10.1016/j.fuproc.2018.04.023

Terashima, N., Kitano, K., Kojima, M., Yoshida, M., Yamamoto, H., and Westermark, U. (2009). "Nanostructural assembly of cellulose, hemicellulose, and lignin in the middle layer of secondary wall of ginkgo tracheid," *Journal of Wood Science* 55, 409-416. https://doi.org/10.1007/s10086-009-1049-x

Tumuluru, J. S. (2018). "Effect of pellet die diameter on density and durability of pellets made from high moisture woody and herbaceous biomass," *Carbon Resources Conversion* 1(1), 44-54. https://doi.org/10.1016/j.crcon.2018.06.002

Wang, J., Minami, E., and Kawamoto, H. (2020). "Thermal reactivity of hemicellulose and cellulose in cedar and beech wood cell walls," *Journal of Wood Science* 66(41). https://doi.org/10.1186/s10086-020-01888-x

Wang, C., Yang, J., Wen, J., Bian, J., Li, M., Peng, F., and Sun, R. (2019). "Structure and distribution changes of Eucalyptus hemicelluloses during hydrothermal and alkaline pretreatments," *International Journal of Biological Macromolecules* 133, 514-521. https://doi.org/10.1016/j.ijbiomac.2019.04.127

Wang, J., Minami, E., Asmadi, M., and Kawamoto, H. (2021). "Thermal degradation of hemicellulose and cellulose in ball-milled cedar and beech wood," *Journal of Wood Science* 67, article 32. https://doi.org/10.1186/s10086-021-01962-y

Wang, S., Dai, G., Ru, B., Zhao, Y., Wang, X., Zhou, J., Luo, Z., and Cen, K. (2016). "Effects of torrefaction on hemicellulose structural characteristics and pyrolysis behaviors," *Bioresources Technology* 218, 1106-1114. https://doi.org/10.1016/j.biortech.2016.07.075

Wang, L., Riva, L., Skreiberg, Ø., Khalil, R., Bartocci, P., Yang, Q., Yang, H., Wang, X., Chen, D., Rudolfsson, M., and Nielsen, H. K. (2020). "Effect of torrefaction on properties of pellets produced from woody biomass," *Energy & Fuels* 34, 15343-15354. https://doi.org/10.1021/acs.energyfuels.0c02671

Werner, K., Pommer, L., and Broström, M. (2014). "Thermal decomposition of hemicelluloses," *Journal of Analytical and Applied Pyrolysis* 110, 130-137. https://doi.org/10.1016/j.jaap.2014.08.013

Yang, W., Su, Y., Dong, G., Qian, G., Shi, Y., Mi, Y., Zhang, Y., Xue, J., Du, W., Shi, T., and Chen, S. (2022). "Liquid chromatography–mass spectrometry-based metabolomics analysis of flavonoids and anthraquinones in *Fagopyrum tataricum* L. Gaertn. (tartary buckwheat) seeds to trace morphological variations," *Food Chemistry* 331, article 127354. https://doi.org/10.1016/j.foodchem.2020.127354

Yeh, T. F., Chang, H. M., and Kadla, J. F. (2004). "Rapid prediction of solid wood lignin content using transmittance near-infrared spectroscopy," *Journal of Agricultural and Food Chemistry* 52(6), 1435-1439. https://doi.org/10.1021/jf034874r

Yoshida, T., Sano, T., Nomura, H., Gensai, H., Watada, S., and Ohara, S. (2013). "Fundamental study on the production of 'hyper wood pellet'—Effect of torrefaction condition on grinding and pelletizing properties," *Journal of Energy Power Engineering* 7, 705-710.

Yoshida, T., Kubojima, Y., Kamikawa, D., Inoue, M., Kiguchi, M., Tanaka, K., Murata, Y., Masui, M., Ohyabu, Y., and Tsuru, T. (2017). "Preliminary production test of torrefied woody biomass fuel in a small scale plant," *Journal of the Japan Institute of Energy* 96, 310-313. https://doi.org/10.3775/jie.96.310

Zaini, I. N., Wen, Y., Mousa, E., Jonsson, P. G., and Yan, W. (2021). "Primary fragmentation behavior of refuse derived fuel pellets during rapid pyrolysis," *Fuel Process Technology* 216, 1106796. https://doi.org/10.1016/j.fuproc.2021.106796

Article submitted: May 12, 2025; Peer review completed; August 15, 2025; Revised version received and accepted: December 26, 2025; Published: January 5, 2026.
DOI: 10.15376/biores.21.1.1548-1563